Chemical Physics Letters 475 (2009) 120–123

Contents lists available at ScienceDirect

Chemical Physics Letters

journal homepage: www.elsevier.com/locate/cplett

Important effects of neighbouring nucleotides on electron induced DNA single-strand breaks

Pierre-François Loos [a,*], Elise Dumont [b], Adèle D. Laurent [a], Xavier Assfeld [a]

[a] Equipe de Chimie et Biochimie Théoriques, UMR 7565 CNRS-UHP, Institut Jean Barriol (FR CNRS 2843), Faculté des Sciences et Techniques, Nancy-Université, B.P. 70239, 54506 Vandœuvre-lès-Nancy, France
[b] Laboratoire de Chimie, UMR 5182 CNRS, Ecole Normale Supérieure de Lyon, 46, allée d'Italie, 69364 Lyon Cedex 07, France

ARTICLE INFO

Article history:
Received 6 May 2009
In final form 19 May 2009
Available online 24 May 2009

ABSTRACT

In this Letter, we present Quantum Mechanics/Molecular Mechanics (QM/MM) calculations on molecules containing a 2-deoxycytidine-3′-monophosphate moiety (3′-dCMPH). In particular, we examine the effect that including neighbouring nucleotides at the Molecular Mechanic (MM) level has on the calculated electron affinities and on the energetic barriers of the C3′–O3′ bond cleavage. Our results demonstrate that the surrounding nucleotides relocate the excess electron from the π^* orbital of the base to a diffuse phosphate-centred orbital, leading to the formation of a dipole-bound anion state. Both the electron affinities and the activation energy of C3′–O3′ bond cleavage are strongly increased.

1. Introduction

Recent experiments [1,2] on supercoiled DNA have demonstrated that low-energy electrons [3] (LEEs) (0.1–2 eV) induce single-strand breaks (SSBs) *via* electron attachment to nucleotides and subsequent sugar–phosphate bond rupture. An in-depth understanding of these lesions is of great importance for the development of improved, more controlled radiotherapy strategies [4]. Chemical pathways leading to SSBs cannot be inferred from experiments, and their determination has also proved to be a real tour-de-force in computational chemistry, requiring state-of-the-art quantum calculations.

The first theoretical explanation was reported by Li et al. based on a sugar–phosphate–sugar (S–P–S) model [5]. They demonstrated that SSBs may occur with an energy barrier of ~10 kcal/mol for C3′–O3′ or C5′–O5′ sugar bond cleavage in gas phase. The authors described the nature of the radical anion species in a later review article [6] and concluded that the initial state was a dipole-bound state.

This seminal work was reinvestigated by Simons and co-workers [7] with inclusion of the nucleobase: they show that the electron attachment is more likely to occur on the base-centred π^* orbital, with an activation barrier in the range 7–15 kcal/mol in gas phase and 13–30 kcal/mol in aqueous solution.

By an exhaustive examination of the electron affinities [8] and energy barriers of C3′–O3′ and C5′–O5′ bond cleavages [9,10] of pyrimidine nucleotides, Gu et al. established that the C3′–O3′ sugar bond rupture in molecules containing 2′-deoxycytidine-3′-monophosphate (3′-dCMPH) is associated with the smallest activation barrier (6.2 kcal/mol) and may therefore dominate the SSBs in DNA [9].

These intensive research efforts on model systems (ca. 30 atoms) have delineated some of the most likely and favourable chemical pathways resulting in SSB. However, the energetic landscapes of such complex systems can be adjusted by many environmental factors: inclusion of adjacent nucleotides, pairing to complementary bases, hydrogen bonding, π stacking, protonation of the phosphate groups, etc. Two energetic quantities govern the ease and selectivity of SSB: (i) the electron affinities that quantify the ease with which electrons are captured, and (ii) the activation barrier needed to cleave a covalent bond. Hybrid Quantum Mechanics/Molecular Mechanics (QM/MM) calculations offer a near-optimal approach to investigate the effect of the surroundings on these two central energetic quantities, and are reported in this Letter.

2. Computational details

We here take advantage of recent developments in our group, within the Local Self-Consistent Field (LSCF) framework that enable the placement of a frontier along a *polarized* bond with no artefact [11–14]. A doubly occupied strictly localized bond orbital (SLBO) is employed to link the QM and the MM parts. QM/MM calculations were performed with our local modified version of the GAUSSIAN 03 package [15] linked to the TINKER software [16] for the MM calculations. Full geometry optimizations were performed. Because of the spatially extended behavior of this phenomenon, the whole nucleotide where the bond cleavage occurs has to be

* Corresponding author. Present address: Research School of Chemistry, Australian National University, Canberra, ACT 0200, Australia.
E-mail address: Pierre-Francois.Loos@cbt.uhp-nancy.fr (P.-F. Loos).

0009-2614/$ - see front matter © 2009 Elsevier B.V. All rights reserved.
doi:10.1016/j.cplett.2009.05.041

included in the QM part. The QM/MM frontiers are located between the C5′ and the O5′ atoms which connect the deoxyribose ring to the phosphate group (Fig. 1). The SLBO is obtained from a preliminary computation on a model molecule (CH_3O–PO_2H–OCH_3) featuring the chemical bond of interest, and subsequently transferred to the oligeonucleotide sequence (single-stranded 5′-CCC-3′ and corresponding double-stranded fragment formed by the association of the 5′-CCC-3′ and 3′-GGG-5′ subunits and hereafter denoted CG–CG–CG). The core electrons of the frontier atoms are taken into account by means of a self-consistent core orbital [17,18] (SCCO): this ensures a proper description of polarized frontier bonds.

The scan along the C3′–O3′ bond has been performed starting from the equilibrium distance of the radical anion and increasing the bond length with a step size of 0.05 Å (*ModRedundant* option of the GAUSSIAN 03 software). The transition states (TS) of model systems have been optimized with the default Berny algorithm. QM/MM initial geometries for single-stranded (ss) 5′-CCC-3′ and the corresponding double-stranded (ds) CG–CG–CG compound have been created with the *nucleic* program of the TINKER software using the conventional geometrical parameters of B-DNA. On the basis of auxiliary calculations on a model system, we have concluded that a protonated phosphate within the QM part is both the most practical and representative way for describing physiological phosphate in gas phase. Then, we will consider the protonated state of the phosphate group in our QM/MM calculations including single-stranded and double-stranded DNA. Moreover, a sodium counter-ion treated at the MM level has been added in the vicinity of each phosphate group located in the MM part (Fig. 1).

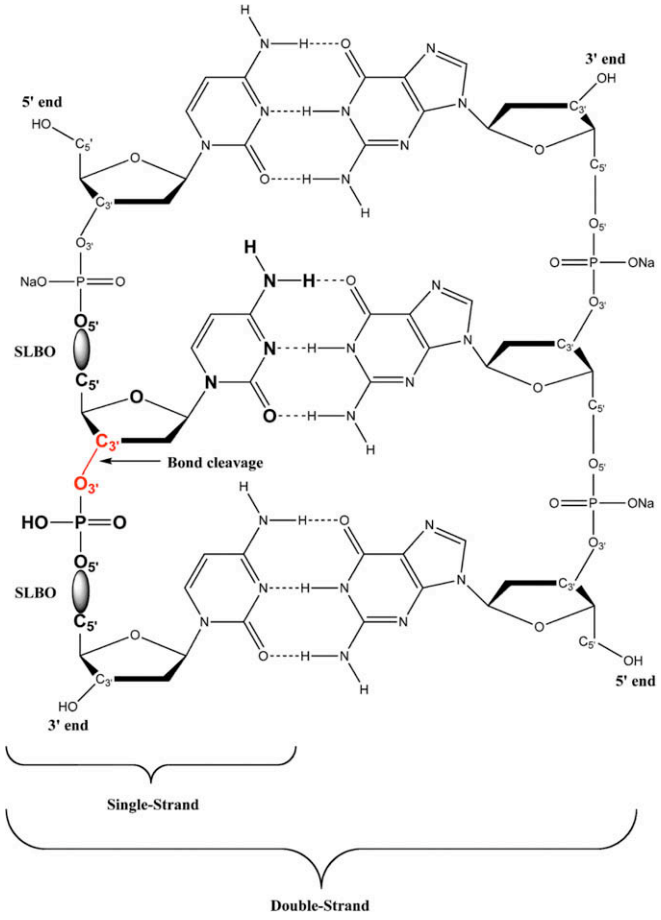

Fig. 1. QM/MM partitioning of ss-3′-dCMPH and ds-3′-dCMPH models. The QM part is depicted in bold and the QM/MM boundaries are located between the C5′ and O5′ atoms of the deoxyribose ring. The strictly localized bond orbitals (SLBO), which define the QM/MM frontiers are also represented.

The MM surrounding is described by the Amber99 force field [19,20]. The van der Waals parameters for the QM atoms are set to the values defined for the corresponding atom type of the force field. One of the decisive advantages of the LSCF approach is that it bypasses the point charge redistribution usually needed to ensure the overall electroneutrality of the MM part. Indeed, possible artefacts in QM/MM calculations could easily arise due to the sensitivity of electron affinities to electrostatic environment.

Concerning the QM calculations, the B3LYP functional was used in conjunction with the 6-311+G* basis set. To take into account solvent effects, the Polarizable Continuum Model (IEF-PCM) with UA0 atomic radii was employed [21]. Adiabatic electron affinities (AEA) are defined as the difference between the total energies of the neutral (N) and radical anion (RA) states at their optimized geometries (AEA = E(N) − E(RA)), while the vertical electron affinities (VEA) and vertical detachment energies (VDE) are defined as the difference between the total energies of the neutral and radical anion states at the neutral and radical anion optimized geometries, respectively.

In order to validate the level of the theory used in the present work (B3LYP/6-311+G*), we have performed an initial analysis of the results obtained on the model system (3′-dCMPH) previously investigated in the literature using the B3LYP/DZP++ approach [2]. The results can be found in Table 1 for the calculations corresponding to the gas phase and the solution. The AEA, VEA and VDE values reported in Ref. [2] are equal to 0.33, 0.15 and 1.28 eV, respectively. Due to the extreme basis-set dependence of these quantities [22], we believe that our results (0.15, 0.00 and 0.87 eV) are consistent with the former investigations. Moreover, the energetic barrier of the C3′–O3′ bond cleavage, obtained with the level of theory we proposed, in both the gas phase and in solvent (6.7 and 14.1 kcal/mol, respectively) are extremely close to the results reported in Ref. [9] at the B3LYP/DZP++ level of theory (6.17 and 12.82 kcal/mol, respectively), leading us to be confident to the ability of our QM theoretical scheme for describing properly SSBs in DNA.

In our implementation, the QM wave function is polarized by the electric field created by the MM point charges, which is referred as electrostatic embedding (EE) in the following. This methodology has been successfully applied to a wide range of chemical problems, such as the determination of absorption properties of grafted azobenzene chromophore [27] and the electron attachments on disulfide-containing proteins [28,29]. One other key point is the mechanical constraint exerted by the neighbouring nucleobases, which can be obtained by entirely switching off the EE of the MM part.

Table 1
Adiabatic electron affinities (AEA), vertical electron affinities (VEA) and vertical detachment energies (VDE) of 3′-dCMPH, ss-3′-dCMPH and ds-3′-dCMPH molecules (in eV). Values in parenthesis correspond to PCM calculations, using water with ε = 78.39 and UA0 radii.

Process	AEA	VEA	VDE
3′-dCMPH → 3′-dCMPH$^-$	0.15 (2.07)	0.00 (1.36)	0.87 (2.44)
ss-3′-dCMPH → ss-3′-dCMPH$^-$	0.80 (2.12)[a]	−0.25 (1.46)[a]	1.50 (2.34)[a]
ss-3′-dCMPH → ss-3′-dCMPH$^-$[b]	0.55	0.00	0.05
ds-3′-dCMPH → ds-3′-dCMPH$^-$	0.92 (1.95)[a]	0.02 (1.63)[a]	1.73 (2.45)[a]
ds-3′-dCMPH → ds-3′-dCMPH$^-$[c]	0.32	0.12	1.02
ds-3′-dCMPH → ds-3′-dCMPH$^-$[b]	−0.24	−0.01	0.02

[a] PCM calculation based on gas phase optimized structure.
[b] Calculations performed without any electrostatic embedding from the neighbouring nucleotides.
[c] Calculations performed without the electrostatic embedding due to the nucleotides of the second strand.

3. Results and discussion

Electron affinities for single-stranded (ss) and double-stranded (ds) DNA are given in Table 1. The AEA are 0.80 and 0.92 eV for ss-3′-dCMPH and ds-3′-dCMPH, respectively, which represent an increase of 0.65 and 0.77 eV compared to the model system 3′-dCMPH (0.15 eV). This proves, without ambiguity, that the ss-DNA and ds-DNA radical anions are electronically stable in gas phase.

It should be noted that the VEA value of ds-3′-dCMPH (0.02 eV) means that it can capture near-0 eV electron in gas phase. This value, which is greater than that of 3′-dCMPH and 0.27 eV higher than that of ss-3′-dCMPH, suggests that the double stranded compound will more easily capture a free electron than ss-DNA or 3′-dCMPH. The positive VDE of ss-3′-dCMPH (1.50 eV) and ds-3′-dCMPH (1.73 eV) radical anion, which determine the energy needed for the detachment of the electron, ensure that the anion is in a stationary state. Consequently, C3′–O3′ bond stretching exists and can lead to the rupture of that bond due to the transfer of the excess electron in the σ^* orbital.

An interesting feature of this process is the location of the excess electron on the 3′-dCMPH moiety, which is not intuitive. A previous study by Schaefer and co-workers [23] on 2-deoxyribonucleotides-3′-5′-diphosphate (3′-5′-dTDP, 3′-5′-dCDP, 3′-5′-dGDP and 3′-5′-dADP) has reported a partial location of the excess electron in the vicinity of the 3′-phosphate group in the gas phase, while studies on both 3′- and 5′-monophosphate radical anions have shown that the excess electron density is not located on the phosphate group [8–10], but on the nucleobase. They conclude that the '*results seem to suggest that introducing a phosphate group at the 3′ or 5′ position of the ribose improves the electron-capturing ability of the 3′-phosphate fragment*' [23].

Our results (Mulliken spin densities on each group, gathered in Table 2) show the formation of an anion centred on the phosphate for ss- and ds-DNA, as revealed by an examination of the shape of the singly occupied molecular orbitals (SOMO) for ss-3′-dCMPH and ds-3′-dCMPH (Fig. 2). We do not attempt to ascertain the nature of the orbital [24–26]. A similar distribution is found in aqueous solution, where the extra negative charges are also located in diffuse (phosphate-centred) orbitals. As the electrostatic embedding (EE) of the nucleotides treated by a classical force field is gradually switched off, about 60% of the excess electron density of ss-3′-dCMPH migrates from the phosphate moiety to the pyrimidine ring. The same phenomenon is observed for the ds-3′-dCMPH molecule: the EE created by the second strand composed by purines partially redistributes the excess electron density (by ca. 25%) from the phosphate moiety to the pyrimidine. This effect is increased when the overall EE is turned off with a total migration of the negative charge from the phosphate to the vicinity of the deoxyribose ring. This leads to an equal distribution of the spin density for each moiety (phosphate, ribose and base). This latter point emphasises the importance of the geometrical modifications induced by the nucleotides from the low-level part [24,28,29]. Indeed, at the same level of theory and for the isolated 3′-dCPMH molecule, the whole excess electron density is located on the base. The mechanical constraint exerted by the environment has the effect to spread out the excess electron density over the three chemical fragments.

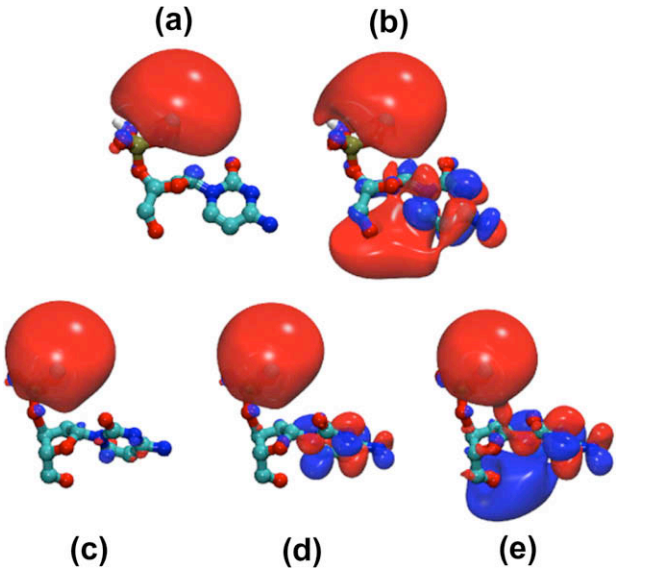

Fig. 2. Evolution of the SOMO of the ss-3′-dCMPH$^-$ (top) and ds-3′-dCMPH$^-$ (bottom) with respect to the electrostatic embedding (EE) created by the other nucleotides ((a) and (c)). For the sake of clarity, only the QM part has been depicted. SOMOs (b) and (e) have been obtained without any electrostatic embedding from the neighbouring nucleotides, while SOMO (d) have been obtained without the electrostatic embedding due to the nucleotides of the second strand.

Table 2
Mulliken spin densities of the phosphate, ribose and base moieties for the radical anion state of 3′-dCMPH, ss-3′-dCMPH and ds-3′-dCMPH (in electron). Values in parenthesis correspond to PCM calculations, using water with $\varepsilon = 78.39$ and UA0 radii.

Moiety	Phosphate	Ribose	Base
3′-dCMPH$^-$	0.07 (0.00)	0.00 (0.01)	0.93 (0.99)
ss-3′-dCMPH$^-$	0.91 (1.04)[a]	0.08 (0.00)[a]	0.02 (−0.04)[a]
ss-3′-dCMPH$^-$[b]	0.45	−0.12	0.67
ds-3′-dCMPH$^-$	0.92 (0.92)[a]	0.02 (0.07)[a]	0.06 (0.01)[a]
ds-3′-dCMPH$^-$[c]	0.77	−0.02	0.25
ds-3′-dCMPH$^-$[b]	0.36	0.27	0.37

[a] PCM calculation based on gas phase optimized structure.
[b] Calculations performed without any electrostatic embedding from the neighbouring nucleotides.
[c] Calculations performed without the electrostatic embedding due to the nucleotides of the second strand.

The excess electron density distribution has a strong impact on electron affinities (Table 1). Indeed, we observe a decrease of the electron affinities when the EE is gradually attenuated. For instance, when the EE of the second strand is turned off, the AEA value of ds-3′-dCMPH decrease by 0.60 eV (from 0.92 to 0.32 eV) and it falls to −0.24 eV when the overall EE is turned off. The latter value is consistent with the results reported in Ref. [8] for the phosphate attached 3′-dCPMH (−0.20 eV) and highlight once again the huge variation of the AEA due to the geometrical modifications. A similar trend is observed for ss-3′-dCMPH.

To estimate the influence of water surrounding [25,30] on ss-DNA and ds-DNA, PCM corrections to electron affinities have been computed based on the gas phase optimized structures. These values are listed in parenthesis in Table 1. Solvation effects strongly reinforce the electron capture ability: the electron affinity values (AEA, VEA and VDE) are very close to the ones for model compounds in aqueous solution for both ss-3′-dCMPH and ds-3′-dCMPH. The ss-DNA and ds-DNA radical anions are then even more stable in aqueous solution. Interestingly enough, in aqueous solution, the negative charge is almost completely located on the 3′-phosphate group (up to 90%) for both ss-3′-dCMPH and ds-3′-dCMPH (see Table 2). This contrasts with the data reported for isolated nucleotides by Schaefer and co-workers [23] on 3′-5′-dCDP radical anion. They observe a relocation of the charge distribution in the vicinity of the nucleobase due to the solvation effects. Both results clearly show the drastic influence of modelling the surrounding accurately [25,30].

Fig. 3 shows the energy profile along the C3′–O3′ reaction coordinates for 3′-dCMPH and ds-3′-dCMPH. Along the C3′–O3′ reaction coordinate, the excess electron is transferred from a

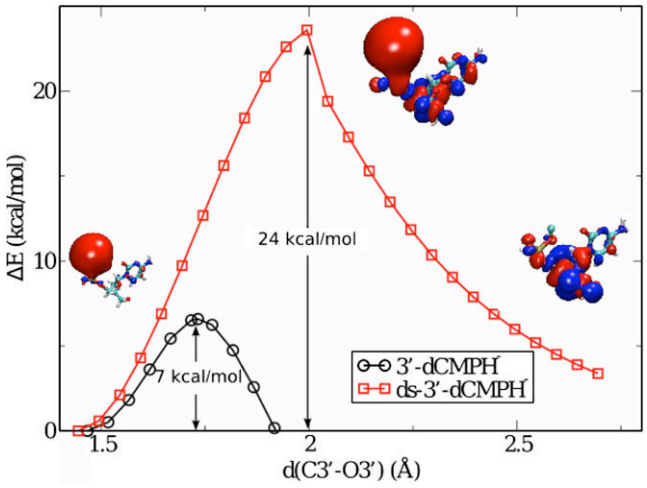

Fig. 3. Scan of the C3′–O3′ bond for 3′-dCMPH$^-$ and ds-3′-dCMPH$^-$. Relative energies of the C3′–O3′ bond cleavage (ΔE) are given in kcal/mol. The SOMOs corresponding to the minimum and maximum along the bond cleavage coordinates, as well as the dissociated product are depicted for ds-3′-dCMPH$^-$.

diffuse phosphate-centred orbital to the σ^* orbital of the C3′–O3′ bond (see SOMO plots on Fig. 3). This yields an activation energy of ~24 kcal/mol for the C3′–O3′ bond cleavage in ds-3′-dCMPH, compared to 6.7 kcal/mol and 14.1 kcal/mol for 3′-dCMPH in the gas phase and in aqueous solution, respectively. In the same way phosphate-based excess electron density increases electron affinities, it also seems to increase the energy barrier of C3′–O3′ bond rupture. This is in agreement with results of Laaksonen and coworkers [31] on 2′-deoxyguanosine-3′-monophosphate molecule (3′-dGMP), which show that the C3′–O3′ energy barrier is higher in gas phase (where the excess electron is partially located near the phosphate group) than in aqueous solution (where it is mainly dipole-bound [6] to the guanine base).

4. Concluding remarks

Our results demonstrate that neighbouring nucleobases induce a dramatic redistribution of the excess electron density from the base-centred π^* orbital to a diffuse orbital of the phosphate group, leading to a dipole-bound anion state. This is associated with an increase in both electron affinity and activation energy of the C3′–O3′ bond cleavage (~24 kcal/mol) compared to 3′-dCMPH (~7 kcal/mol). Not only the electronic polarization induced by the surroundings is important, but we shown that the geometrical modifications created by the neighbouring bases have an important effect. This shed light on the importance of taking into accounts the surrounding to achieve comprehensive pictures of SSB in DNA.

Acknowledgements

The authors are grateful to Dr. Nicolas Ferré (Université Aix-Marseille I, France) for providing parts of the code. They also acknowledge financial support from the Jean Barriol Institute (FR CNRS 2843). One of us (PFL) thanks the ANU Research School of Chemistry for a postdoctoral fellowship. He also thanks Yves Bernard and Dr. Deb Crittenden for helpful comments on the manuscript, and fruitful discussions.

References

[1] B. Boudaiffa, P. Cloutier, D. Hunting, M.A. Huels, L. Sanche, Science 287 (2000) 1658.
[2] F. Martin, P.D. Burrow, A. Cai, P. Cloutier, D. Hunting, L. Sanche, Phys. Rev. Lett. 93 (2004) 068101.
[3] L. Sanche, Eur. Phys. J. D 35 (2005) 367.
[4] J.A. LaVerne, S.M. Pimblott, Radiat. Res. 141 (1995) 208.
[5] X. Li, M.D. Sevilla, L. Sanche, J. Am. Chem. Soc. 125 (2003) 13668.
[6] X. Li, M.D. Sevilla, Adv. Quantum Chem. 52 (2007) 59.
[7] J. Simons, Acc. Chem. Res. 39 (2006) 772.
[8] J. Gu, J. Wang, H.F. Schaefer III, J. Am. Chem. Soc. 128 (2006) 1250.
[9] J. Gu, J. Wang, J. Leszczynski, J. Am. Chem. Soc. 128 (2006) 9322.
[10] X. Bao, J. Gu, J. Wang, J. Leszczynski, Proc. Natl. Acad. Sci. USA 103 (2006) 5658.
[11] X. Assfeld, J.-L. Rivail, Chem. Phys. Lett. 263 (1996) 100.
[12] N. Ferré, X. Assfeld, J.-L. Rivail, J. Comput. Chem. 23 (2002) 610.
[13] Y. Moreau, P.-F. Loos, X. Assfeld, Theor. Chem. Acc. 112 (2004) 228.
[14] P.-F. Loos, X. Assfeld, J. Chem. Theor. Comput. 3 (2007) 1047.
[15] M.J. Frisch et al., Gaussian 03, Revision B.05, Gaussian, Inc., Wallingford, CT, 2004.
[16] J.W. Ponder, Tinker, Version 4.2, Washington University, St. Louis, MO, 2004.
[17] A. Fornili, P.-F. Loos, M. Sironi, X. Assfeld, Chem. Phys. Lett. 427 (2006) 236.
[18] P.-F. Loos, A. Fornili, M. Sironi, X. Assfeld, Comput. Lett. 4 (2007) 473.
[19] W.D. Cornell et al., J. Am. Chem. Soc. 117 (1995) 5179.
[20] J. Wang, P. Cieplak, P.A. Kollman, J. Comput. Chem. 21 (2000) 1049.
[21] J. Tomasi, B. Mennucci, R. Cammi, Chem. Rev. 105 (2005) 2999.
[22] J.C. Rienstra-Kiracofe, G.S. Tschumper, H.F. Schaefer III, S. Nand, G.B. Ellison, Chem. Rev. 102 (2002) 231.
[23] J. Gu, Y. Xie, H.F. Schaefer III, Nucleic Acids Res. 35 (2007) 5165.
[24] P.D. Burrow, G.A. Gallup, A. Modelli, J. Phys. Chem. A 112 (2008) 4106.
[25] A. Kumar, M.D. Sevilla, J. Phys. Chem. B 111 (2007) 5564.
[26] A. Kumar, M.D. Sevilla, J. Am. Chem. Soc. 130 (2008) 2130.
[27] P.-F. Loos, J. Preat, A.D. Laurent, C. Michaux, D. Jacquemin, E.A. Perpete, X. Assfeld, J. Chem. Theor. Comput. 4 (2008) 637.
[28] E. Dumont, P.-F. Loos, A.D. Laurent, X. Assfeld, J. Chem. Theor. Comput. 4 (2008) 1171.
[29] E. Dumont, A.D. Laurent, P.-F. Loos, X. Assfeld, J. Chem. Theor. Comput. (2009), doi:10.1021/ct900093h.
[30] A. Kumar, M.D. Sevilla, S. Suhai, J. Phys. Chem. B 112 (2008) 5189.
[31] P. Schyman, A. Laaksonen, J. Am. Chem. Soc. 130 (2008) 12254.